Dissertation_thesis_CS2327__Copy___Copy_.pdf

Indian Statistical Institute

Document Details

Submission ID
trn:oid:::3618:142751146

Submission Date
Jun 12, 2026, 1:01 PM GMT+5:30

Download Date
Jun 12, 2026, 1:11 PM GMT+5:30

File Name
Dissertation_thesis_CS2327__Copy___Copy_.pdf

File Size
5.4 MB

51 Pages

11,208 Words

58,071 Characters

8% Overall Similarity

The combined total of all matches, including overlapping sources, for each database.

Filtered from the Report

- Bibliography

Match Groups

95 Not Cited or Quoted 8%
Matches with neither in-text citation nor quotation marks

1 Missing Quotations 0%
Matches that are still very similar to source material

0 Missing Citation 0%
Matches that have quotation marks, but no in-text citation

0 Cited and Quoted 0%
Matches with in-text citation present, but no quotation marks

Top Sources

6% Internet sources
7% Publications
0% Submitted works (Student Papers)

Integrity Flags

0 Integrity Flags for Review

No suspicious text manipulations found.

Our system's algorithms look deeply at a document for any inconsistencies that would set it apart from a normal submission. If we notice something strange, we flag it for you to review.

A Flag is not necessarily an indicator of a problem. However, we'd recommend you focus your attention there for further review.

Match Groups

- **95** Not Cited or Quoted 8%
  Matches with neither in-text citation nor quotation marks
- **1** Missing Quotations 0%
  Matches that are still very similar to source material
- **0** Missing Citation 0%
  Matches that have quotation marks, but no in-text citation
- **0** Cited and Quoted 0%
  Matches with in-text citation present, but no quotation marks

Top Sources

6% Internet sources
7% Publications
0% Submitted works (Student Papers)

Top Sources

The sources with the highest number of matches within the submission. Overlapping sources will not be displayed.

1	Internet	download.bibis.ir 2%
2	Internet	arxiv.org 1%
3	Publication	Habib M. Ammari. "Theory and Practice of Wireless Sensor Networks: Cover, Sens... <1%
4	Publication	Habib M. Ammari, Frank H. Dotterweich. " A Computational Geometry-Based App... <1%
5	Publication	Shende, Dipika Sarjerao. "Joint Reconfigurable Intelligent Surface Selection and F... <1%
6	Internet	technodocbox.com <1%
7	Internet	hdl.handle.net <1%
8	Publication	Jingsen Liu, Hao Wu, Yu Li, Ping Hu. "A multi-mechanism improved flow direction ... <1%
9	Internet	theses.hal.science <1%
10	Internet	konyvtar.uni-pannon.hu <1%

11 Internet

www.maths.ed.ac.uk <1%

12 Publication

"Advanced Information Networking and Applications", Springer Science and Busi... <1%

13 Internet

pure.au.dk <1%

14 Internet

sciencedocbox.com <1%

15 Publication

Quan La Van, Thai Tran Quoc, Cuong Van Duc, Minh Nguyen Dinh Tuan, Son Nguy... <1%

16 Publication

Aparajita Chowdhury, Debashis De. "Energy-efficient coverage optimization in wi... <1%

17 Internet

drops.dagstuhl.de <1%

18 Internet

www.tandfonline.com <1%

19 Publication

Signals and Communication Technology, 2014. <1%

20 Internet

etheses.dur.ac.uk <1%

21 Internet

d-nb.info <1%

22 Internet

export.arxiv.org <1%

23 Internet

link.springer.com <1%

24 Publication

"Magnetic Techniques for the Treatment of Materials", Springer Science and Busi... <1%

25	Publication	Habib M. Ammari. "Connected k-coverage in two-dimensional wireless sensor net... <1%
26	Publication	Kalyan Nakka, Habib M. Ammari. "An energy-efficient irregular hexagonal tessell... <1%
27	Internet	doczz.net <1%
28	Internet	www.mdpi.com <1%
29	Internet	wwwhome.math.utwente.nl <1%
30	Publication	Habib M. Ammari. " A Computational Geometry-based Approach for Planar -Cove... <1%
31	Publication	Kalyan Nakka, Habib M. Ammari. "Hierarchical Deployment and Square Tessellati... <1%
32	Publication	Kalyan Nakka, Habib M. Ammari. "k-CSqu: Ensuring connected k-coverage using c... <1%
33	Internet	encyclopedia.pub <1%
34	Internet	fedorvf.github.io <1%
35	Internet	www.sce.carleton.ca <1%
36	Publication	"The Art of Wireless Sensor Networks", Springer Science and Business Media LLC, ... <1%
37	Publication	Aparajita Chowdhury, Debashis De. "FIS-RGSO: Dynamic Fuzzy Inference System ... <1%
38	Publication	Solomon W. Golomb, Andy Liu. "Solomon Golomb's Course on Undergraduate Co... <1%

An Efficient Hierarchical Deployment Of Sensors For K-coverage In Planner Wireless Sensor Network

A dissertation submitted in partial fulfilment for the degree of

Master of Technology

in

Computer Science

by

Abhay Raj Singh
Roll no. - **CS2401**

under the supervision of

Professor Sasthi C. Ghosh
Advanced Computing and Microelectronics Unit
(ACMU)

INDIAN STATISTICAL INSTITUTE, KOLKATA

June 2026

Declaration

Abhay Raj Singh, with Roll No. **CS2401**, hereby declare that the material presented in the dissertation titled **An Efficient Hierarchical Deployment Of Sensors For K-coverage In Planner Wireless Sensor Network** represents original work carried out by me for the degree of **Master of Technology in Computer Science** at the **Indian Statistical Institute, Kolkata**.

Furthermore, I affirm that no sections of this report have been sourced or copied from external references without proper attribution. I am aware that any instances of plagiarism or the use of unacknowledged materials from third parties will be treated with the utmost seriousness and consequences.

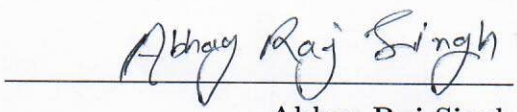

Abhay Raj Singh
M.Tech (CS), CS2401
Indian Statistical Institute
Kolkata – 700108, India

CERTIFICATE

This is to certify that the dissertation entitled **"An Efficient Hierarchical Deployment Of Sensors For K-coverage In Planner Wireless Sensor Network"** submitted by **Abhay Raj Singh** to the **Indian Statistical Institute, Kolkata**, in partial fulfillment of the requirements for the degree of **Master of Technology in Computer Science**, is an authentic and genuine record of the research work carried out by the candidate under my supervision and guidance. I affirm that the dissertation has met all the necessary requirements in accordance with the regulations of this institute.

Professor Sasthi C. Ghosh
ACMU Unit
Indian Statistical Institute
Kolkata – 700108, India

iThenticate Page 8 of 56 - Integrity Submission Submission ID trn:oid:::3618:142751146

Acknowledgements

I would like to express my heartfelt gratitude to **Dr. Sasthi C. Ghosh**, my advisor at the *Advanced Computing and Microelectronics Unit* of the **Indian Statistical Institute, Kolkata**, for his invaluable guidance, constant support, and inspiration. His deep knowledge and insightful suggestions have not only enriched this work but also shaped my approach to research.

My sincere thanks go to **Lakshmikanta Sau**, Senior Research Fellow at the **Indian Statistical Institute**, for his crucial help in gathering key information and for consistently offering valuable ideas and encouragement throughout this project.

I am truly thankful to all the faculty members at the **Indian Statistical Institute** for their insightful teaching and guidance, which have provided essential perspectives for my research.

Finally, I extend my deepest appreciation to my parents and extended family for their unwavering encouragement. I am also grateful to all my friends for their consistent support and motivation. My sincere thanks to everyone who has contributed to this journey, even if I may have unintentionally omitted their names.

Abstract

Ensuring reliable sensing coverage is a fundamental challenge in wireless sensor networks (WSNs), particularly when multiple sensors are monitoring each location to provide robustness against node failures. In this work, we address the problem of deterministic k-coverage in planar WSN by proposing a hierarchical triangular lattice-based deployment strategy that organizes sensor locations across different refinement levels and guarantees coverage of every point in the sensing domain by at least k sensors. Each lattice is three-colorable, and selective activation of color classes ensures adjustable coverage guarantees. We prove that activating a single color class at refinement level t guarantees at least 4^t-coverage inside a triangular region. Using a base-4 decomposition of the required coverage level k, we construct a deployment scheme that achieves arbitrary k-coverage while minimizing the number of sensors. For finite irregular hexagonal (IRH) domain, we drive closed-form expressions for the exact number of sensors and minimum sensor spacing required to ensure k-coverage. Analytical comparison with existing IRH edge-overlap, IRH inner-diamond and square-band based deployment strategies show that the proposed method either reduces the required number of sensors or increases the minimum sensor spacing while maintaining the similar coverage guarantees. The analytical results are also validated against extensive simulations. The proposed framework provides a constructive and scalable approach for efficient sensor deployment in large-scale wireless sensing systems.

Contents

Chapter 1

Introduction

The deployment of sensors in a wireless sensor network (WSN) for uses like environmental monitoring has received a lot of attention lately. Nowadays, WSNs are a reality, and by 2029, global Internet of things (IoT) connections are expected to reach over 38.9 billion [1]. WSN consists of numerous small, low-power sensor nodes equipped with sensing units, transceivers, actuators, limited on-board processing capabilities, and wireless communication functionality [13, 2]. These nodes collaboratively collect, process, and transmit data from their surrounding environment [5]. WSN technology has many advantages over traditional networking technologies, including cheaper costs, scalability, precision, dependability, flexibility, and ease of deployment, which allow it to be used in a variety of different applications [5]. As technology develops and sensors become more intelligent, compact, and affordable, billions of wireless sensors are being used in many applications. The environment monitoring, healthcare, and security are a few possible application areas [10, 11, 9]. Sensor nodes can be used in the military to find, track, or identify hostile movements. Sensor nodes have the ability to perceive and detect their surroundings in order to predict natural disasters before they happen.

The monitored environment significantly influences the network's size, topology, and deployment strategy. Note that a sensor has a fixed sensing area and a limited lifetime [12]. However, a sensor may not function properly due to certain technical issues or unavoidable conditions. In those cases, we cannot solely depend on a particular sensor. As a result, we have to go for the multiple coverage and in general k-coverage [14], where each point in the field of interest (FOI) must be covered by at least k sensors. Note that the choice of k depends on the application at hand. More severe reliability needs are represented by higher values of k, whereas less demanding ones are represented by lower values [15].

A point in the FOI is covered by a sensor if the point lies within the sensing radius of that sensor. Many applications need that at least k sensors, where k is a positive number, cover every point in the FOI. In 1-coverage, each point in the FOI is covered by at least one sensor. In general in k-coverage, $k \geq 1$, each point in the FOI is covered by at least k different sensors. It should be noted that the application for which this WSN is being built determined the value of k. Here, k-coverage is necessary for several applications, including intrusion detection and battlefield surveillance, which helps to increase data availability to assure improved robustness.

To cover a specific FOI, the authors in [4] suggested a bound on the sensor density. A sensor deployment approach was proposed in [3], wherein the sensors were placed inside regular hexagons randomly with a specific side length to cover the entire region, which results in unnecessary wastage of resources. Furthermore, sensor mobility may be required to achieve a specific type of coverage called on demand k-coverage, which requires the sensors to move within a FOI and k-cover them. Regardless of the type of coverage requested by the sensing application, it is essential to lower the total number of active sensors in order to k-cover the FOI.

The coverage problem is similar to the tiling problem, a simple yet difficult problem in elementary geometry on the Euclidean plane. Deploying k sensors on each of the chosen places after obtaining the 1-coverage is one method of reaching k-coverage. However, from an application perspective, this method is not recommended because sensors need to maintain a minimum distance from one another. This is due to the fact that in such a deployment, all of these colocated sensors will not function if a problem occurs at some point. Therefore, optimizing this minimal space between sensors is crucial in addition to lowering sensor density.

The authors in [7] consider a diamond shape area and place k sensors inside it. This provides k-coverage to an irregular hexagonal (IRH) area. They then use that IRH to tile the entire triangular lattice. In order to cover the entire region, the study in [3] proposed a sensor deployment strategy in which k sensors were positioned at the common edge of two neighboring regular hexagons with a given side length for k-covering an irregular hexagonal block. They then tile the entire lattice using that block. The authors of [8] considered a square tessellation of the FOI and sensors with heterogeneous sensing radii for k-coverage of a diamond-shaped block. The diamond-shaped block is then used to tile the FOI.

In order to cover the entire region, the study in [3] proposed a sensor deployment strategy in which k sensors were positioned at the common edge of two neighboring regular hexagons with a given side length for k-covering an irregular hexagonal block.

They then tile the entire lattice using that block. The authors of [8] considered a square tessellation of the FOI and sensors with heterogeneous sensing radii for k-coverage of a diamond-shaped block. The diamond-shaped block is then used to tile the FOI. The existing k-coverage deployment strategies exhibit an inherent tradeoff between sensor density and sensor spacing. In [3] and [7] the suggested deployment achieves k-coverage by concentrating sensors within increasingly compact regions, which leads to severe sensor clustering and rapidly decreasing minimum sensor spacing. On the other side, deployment suggested in [8] preserves larger spacing but the resulted sensor density depends heavily on the ratio of maximum and minimum sensing radii.

Motivated by these limilations, we propose a unique deterministic and structured sensor deployment strategy for achieving k-coverage in planar wireless sensor networks. The proposed method is based on a triangular lattice structure, which is refined across multiple levels to control coverage. By exploiting the three-colorable property of the triangular lattice [6], we show that each refinement level contributes coverage at a different scale. These contributions are combined using a base-4 representation of the required coverage k, allowing flexible and precise control over coverage. To make sure that sensors placed at different refinement levels maintain sufficient spacing, we proposed a centroid-based approach to connect different refinement levels together to provide k-coverage. This ensures non-overlapping multi-level deployment without compromising the coverage guarantee while maintaing sufficient sensor spacing. We derived the closed-form expression for the number of sensors and the minimum sensor spacing required to achieve k-coverage over a certain finite IRH as a FOI. The derived expressions are also validated against extensive simulations. We compare our proposed deployment strategy with three current existing benchmarks [3] [8] [7] in terms of the number of sensors needed, sensor density, and minimum sensor spacing. We find that our approach either produced less sensor density or more sensor spacing in comparison to them.

Section 2 introduces the necessary definitions and presents the system model. In Section 3, we present the method for selecting refinement levels and its corresponding color classes. In Section 4, we propose the centroid based hierarchical sensor deployment strategy. Furthermore, in Section 5, we derive the expressions for sensor density and sensor spacing requirements. In Section 6, we derive the closed-form expressions for the number of sensors for k-coverage for a specific irregular region, and Section 7 compares our proposed approach with the existing benchmarks. The numerical results are presented in Section 8, and concluding remarks are given in Section 9.

Chapter 2

System Model and Preliminaries

This section introduces key terminologies and the network model utilized throughout the work.

2.1 Definitions

(Regular polygon) : A regular polygon is a closed, planar figure bounded by a finite number of straight line segments of equal length, with all interior angles being equal. (Regular polygon tiling) : A tiling, or tessellation, of the Euclidean plane is a collection of sets (tiles) that cover the plane without gaps or overlaps. When the tiles are exclusively regular polygons, the configuration is termed a regular polygon tiling.

(Irregular polygon $H(x, z, y)$) : An irregular polygon $H(x, z, y)$ is a lattice-aligned hexagon that is symmetric around the horizontal axis and made up of equilateral triangular units with alternating side lengths x, z, and y an illustrated in Fig 3.1.

(Irregular polygon tiling) : A tessellation of the Euclidean plane using irregular polygons without gaps or overlaps.

(Cover set) : A cover set for the Euclidean plane is a collection of regular (irregular) polygons such that every point in the plane lies within at least one polygon in the set. (k-coverage set) : A cover set is defined as a k-coverage set if every point in the trianguler lattice is within the sensing range of atleast k different sensors. (Sensing range) : The sensing range of a node is defined as the circular region of radius r around it, within which the sensor can reliably monitor a specified physical or environmental attribute. (Communication range) : The communication range for a sensor node is the maximum possible distance over which it can have a direct, reliable communication link with another node in the network.

(Adjacent polygons) : Two irregular polygons with identical parameters are considered adjacent if they share a common edge.

(Overlapping polygons) : Two irregular polygons of identical parameters are considered overlapping if the intersection of their interior regions is non-empty.

[Triangular lattice] A triangular lattice is a regular arrangement of points in the plane such that the points form a tiling of equilateral triangles, with each point having six equidistant neighbors. We consider a hierarchy of lattices $\{L_t\}$ obtained by uniform refinement.

[3-colorability] A triangular lattice is three-colorable if its vertices can be assigned three colors such that no two adjacent vertices share the same color. Equivalently, each triangle has one vertex of each color. The coloring is invariant under permutation of colors.

[Color classes] The vertices of a three-colorable triangular lattice can be partitioned into three disjoint sets, called color classes, denoted by A, B, and C. Each class contains vertices of the same color, and activating a class corresponds to placing sensors at its vertices.

In this section, we propose a sensor deployment strategy to provide k-coverage requirements over a finite planar domain. In this context, we adopt a geometry-based deterministic approach instead of random deployment. Let us consider that $H(x, z, y)$ be a FOI, and we embed it onto a triangular lattice such that all six vertices of it coincide with lattice vertices. The side length of this hexagon will be determined using lattice parameters corresponding to the dimension of $H(x, z, y)$. Now, the triangular lattice structure is refined hierarchically across multiple levels, where each refinement increases the density of lattice vertices. In a triangular lattice, sensors are positioned at specific lattice vertices at various refinement levels to make use of the three colorable structures in accordance with the necessary coverage k.

2.2 Network Model

We consider $H(x, z, y)$ as a FOI that is covered by a tessellation of equilateral triangles with side r_0. Let L_0 represent the coarse (level-0) triangular lattice and a 3-coloring (1, 2, 3) of it, with side length of triangle r_0, as shown in Fig. 3.2. Therefore, to provide complete k-coverage may require different refined levels of a triangular lattice. For each integer $t \geq 1$, we obtain a refined lattice L_t by subdividing each side of the triangle in L_0 into 2^t equal parts. That result in getting a different refined level lattice with a triangle side length of $a_t = \frac{r_0}{2^t}$. Let L_1 represent level-1 triangular lattice and

a 3-coloring (colors a, b, c) of it, with side length of triangle $\frac{r_0}{2}$, as shown in Fig. 3.3. Note that all sensors are assumed to be homogeneous with a sensing radius of $R = r_0$, and they will be placed only at lattice vertices of one or more refined levels.

2.3 Single Layer Sensor Deployment

Let T be an equilateral triangle of side length r_0. If a sensor with a sensing radius $R = r_0$ is placed at any point within T, then each point of T is covered by that sensor.

The farthest point in T from any vertex is the opposite vertex at a distance of r_0. Since the sensing radius is $R = r_0$, so every point in triangle T is within the sensing range of each active sensor. Therefore, the coverage equals the number of active sensors in triangle T.

Limitation of Single Layer Deployment. If sensors are placed at a single lattice level L_t only, the achievable coverage k is limited by the number of active color classes in L_t. In particular, activating zero, one, two, or three color classes in L_t yields to zero, 4^t, $2 \cdot 4^t$, and $3 \cdot 4^t$, coverage respectively.

Thus, the possible coverage values are restricted by

$$\{0, 4^t, 2 \cdot 4^t, 3 \cdot 4^t\}.$$

This suggests that a single lattice cannot be sufficient for any arbitrary value of k and only offers limited control over k-coverage. For instance, with single lattice level we can't give coverage $k = 5$, 6, or 7.

Activating a single color class (A) on a refinement level L_t guarantees at least 4^t-coverage everywhere within each coarse triangle of side r_0, and activating two (A, B) and three (A, B, C) color classes guarantees 2×4^t-coverage and 3×4^t-coverage, respectively.

Consider a coarse triangle $T \in L_0$ with side length r_0.

1. Subdivision: At refinement level t, each side of T is subdivided into 2^t equal segments. This geometric subdivision results in the creation of $(2^t)^2 = 4^t$ smaller equilateral triangles of side length $a_t = \frac{r_0}{2^t}$ within T.

2. Vertex Density and Coloring: The triangular lattice is three-colorable, meaning its vertices can be partitioned into three disjoint sets A, B, and C. In a refined lattice L_t, the total number of vertices associated with the area of a single coarse

triangle T increases quadratically. Specifically, each color class contributes exactly 4^t vertices that lie within or on the boundary of the coarse triangle T.

3. Coverage Invariance: Every sensor placed at any vertex of L_t maintains a constant sensing radius $R = r_0$. According to Lemma 1, any sensor located at a vertex of the refined lattice L_t that is within or on the boundary of T covers the entire area of T because its distance to any point $p \in T$ is $\leq r_0$.

4. Single Class Activation: By activating a color class, we place 4^t sensors such that each one covers every point in T.

5. Multi-class Activation: Since the color classes A, B, and C are disjoint, activating all three classes is equivalent to summing their individual coverage contributions. Therefore, by activating one, two and three color classes we get the guaranteed k-coverage for $k = 4^t, 2 \times 4^t, 3 \times 4^t$, respectively.

This concludes the proof.

This theorem encourages the use of several refinement levels, each of which provides coverage at a different scale, allowing to achieve k-coverage for any k.

2.4 Multi-layer sensor deployment

10

For every positive integer $k \geq 1$, there exists a finite selection of color classes across a finite set of refinement levels $\{L_t \mid t = 0, 1, \ldots, T\}$ such that placing sensors only at the selected lattice vertices guarantees at least k-coverage everywhere in the domain.

We know that every positive integer k can be uniquely expressed in base 4 as

$$k = \sum_{t=0}^{T} d_t \, 4^t, \qquad d_t \in \{0, 1, 2, 3\}. \tag{2.1}$$

From Theorem 3.2, for each refinement level $\mathcal{L}_t$, choose exactly d_t color classes among $\{A, B, C\}$ and place sensors at every vertex of the chosen colors. If $d_t = 0$, no vertices are selected from $\mathcal{L}_t$.

By Theorem 1, each chosen color class on $\mathcal{L}_t$ contributes at least 4^t to the minimum guaranteed coverage. Summing these contributions over all levels yields

$$\text{Guaranteed coverage} \;\geq\; \sum_{t=0}^{T} d_t 4^t \;=\; k,$$

where T is the number of refinement levels.

Computing Finite Refinement Depth T: The number of refinement levels depends on the required coverage k.

For a given k, we construct refinement levels up to

$$T = \lfloor \log_4 k \rfloor . \tag{2.2}$$

Thus, the deployment uses the collection of different refined lattices $\{L_0, L_1, \ldots, L_T\}$, where lattice L_T represents a triangular lattice structure with vertex spacing $r_0/2^T$. Thus, every integer k is realizable by an appropriate selection of color classes across refinement levels as described below.

Selecting refinement levels and color classes: Given a desired coverage level k:

1. Express k in base 4 as $k = \sum_{t=0}^{T} d_t 4^t$, with $d_t \in \{0, 1, 2, 3\}$.
2. For each t, activate d_t distinct color classes on L_t (e.g., choose A, B, C in order as needed).
3. Place sensors at every vertex of the selected color classes.

It is now evident that the *superimposition* of the selected refinement levels and their corresponding color classes will guarantee the k-coverage everywhere in the interior of the domain.

However, if multiple lattice levels are directly overlaid, some vertices from different refinement levels may coincide. In such cases, multiple sensors would need to be placed at the same location, which is undesirable and leads to inefficient deployment. To support this, in the following section, we propose a centroid-based hierarchical superimposition strategy. Our objective is to provide a superimposition such that the minimum distance δ_{min} between any two sensors is as large as possible.

Chapter 3

Proposed Strategy

In this section, we propose a sensor deployment strategy to provide k-coverage requirements over a finite planar domain. In this context, we adopt a geometry-based deterministic approach instead of random deployment. Let us consider that $H(x, z, y)$ be a FOI, and we embed it onto a triangular lattice such that all six vertices of it coincide with lattice vertices. The side length of this hexagon will be determined using lattice parameters corresponding to the dimension of $H(x, z, y)$. Now, the triangular lattice structure is refined hierarchically across multiple levels, where each refinement increases the density of lattice vertices. In a triangular lattice, sensors are positioned at specific lattice vertices at various refinement levels to make use of the three colorable structures in accordance with the necessary coverage k.

3.1 Network Topology

We consider $H(x, z, y)$ as a FOI that is covered by a tessellation of equilateral triangles with side r_0. Let L_0 represent the coarse (level-0) triangular lattice and a 3-coloring (1, 2, 3) of it, with side length of triangle r_0, as shown in Fig. 3.2. Therefore, to provide complete k-coverage may require different refined levels of a triangular lattice. For each integer $t \geq 1$, we obtain a refined lattice L_t by subdividing each side of the triangle in L_0 into 2^t equal parts. That result in getting a different refined level lattice with a triangle side length of $a_t = \frac{r_0}{2^t}$. Let L_1 represent level-1 triangular lattice and a 3-coloring (colors a, b, c) of it, with side length of triangle $\frac{r_0}{2}$, as shown in Fig. 3.3. Note that all sensors are assumed to be homogeneous with a sensing radius of $R = r_0$, and they will be placed only at lattice vertices of one or more refined levels. In the following subsection, we will discuss a novel sensor deployment strategy for different layers.

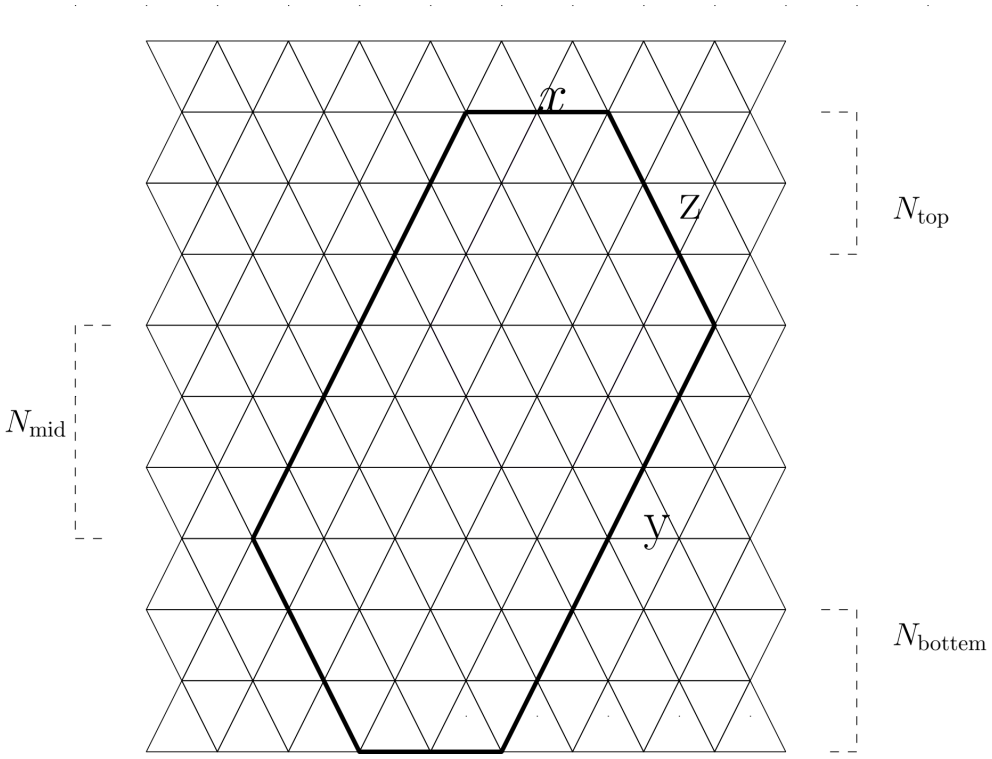

Figure 3.1: Finite FOI $H(x, z, y)$

3.2 Single Layer Sensor Deployment

Let T be an equilateral triangle of side length r_0. If a sensor with a sensing radius $R = r_0$ is placed at any point within T, then each point of T is covered by that sensor.

The farthest point in T from any vertex is the opposite vertex at a distance of r_0. Since the sensing radius is $R = r_0$, so every point in triangle T is within the sensing range of each active sensor. Therefore, the coverage equals the number of active sensors in triangle T.

Limitation of Single Layer Deployment. If sensors are placed at a single lattice level L_t only, the achievable coverage k is limited by the number of active color classes in L_t. In particular, activating zero, one, two, or three color classes in L_t yields to zero, 4^t, $2 \cdot 4^t$, and $3 \cdot 4^t$, coverage respectively.

Thus, the possible coverage values are restricted by

$$\{0, 4^t, 2 \cdot 4^t, 3 \cdot 4^t\}.$$

This suggests that a single lattice cannot be sufficient for any arbitrary value of k and

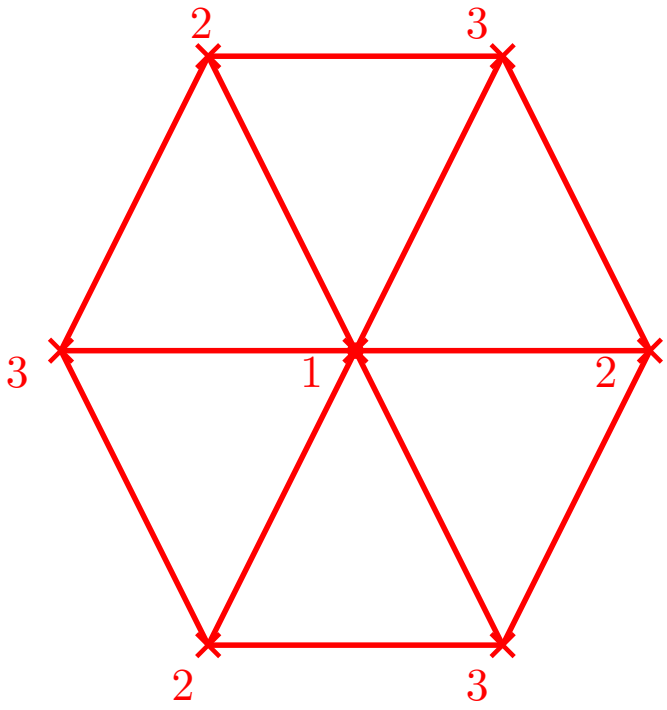

Figure 3.2: L_0: 3-coloring (colors 1, 2, 3) of triangular lattice with side r_0

only offers limited control over k-coverage. For instance, with single lattice level we can't give coverage $k = 5$, 6, or 7.

Activating a single color class (A) on a refinement level L_t guarantees at least 4^t-coverage everywhere within each coarse triangle of side r_0, and activating two (A, B) and three (A, B, C) color classes guarantees 2×4^t-coverage and 3×4^t-coverage, respectively.

Consider a coarse triangle $T \in L_0$ with side length r_0.

1. Subdivision: At refinement level t, each side of T is subdivided into 2^t equal segments. This geometric subdivision results in the creation of $(2^t)^2 = 4^t$ smaller equilateral triangles of side length $a_t = \frac{r_0}{2^t}$ within T.

2. Vertex Density and Coloring: The triangular lattice is three-colorable, meaning its vertices can be partitioned into three disjoint sets A, B, and C. In a refined lattice L_t, the total number of vertices associated with the area of a single coarse triangle T increases quadratically. Specifically, each color class contributes exactly 4^t vertices that lie within or on the boundary of the coarse triangle T.

3. Coverage Invariance: Every sensor placed at any vertex of L_t maintains a constant sensing radius $R = r_0$. According to Lemma 1, any sensor located at a vertex

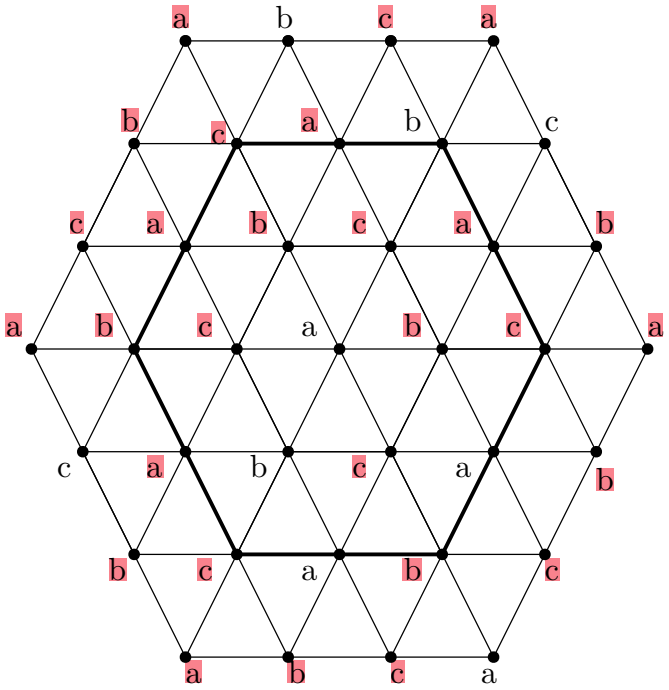

Figure 3.3: L_1: 3-coloring (colors a, b, c) of triangular lattice with side $\frac{r_0}{2}$

of the refined lattice L_t that is within or on the boundary of T covers the entire area of T because its distance to any point $p \in T$ is $\leq r_0$.

4. Single Class Activation: By activating a color class, we place 4^t sensors such that each one covers every point in T.

5. Multi-class Activation: Since the color classes A, B, and C are disjoint, activating all three classes is equivalent to summing their individual coverage contributions. Therefore, by activating one, two and three color classes we get the guaranteed k-coverage for $k = 4^t, 2 \times 4^t, 3 \times 4^t$, respectively.

This concludes the proof.

This theorem encourages the use of several refinement levels, each of which provides coverage at a different scale, allowing to achieve k-coverage for any k.

3.3 Multi-layer sensor deployment

For every positive integer $k \geq 1$, there exists a finite selection of color classes across a finite set of refinement levels $\{L_t \mid t = 0, 1, \ldots, T\}$ such that placing sensors only at the selected lattice vertices guarantees at least k-coverage everywhere in the domain.

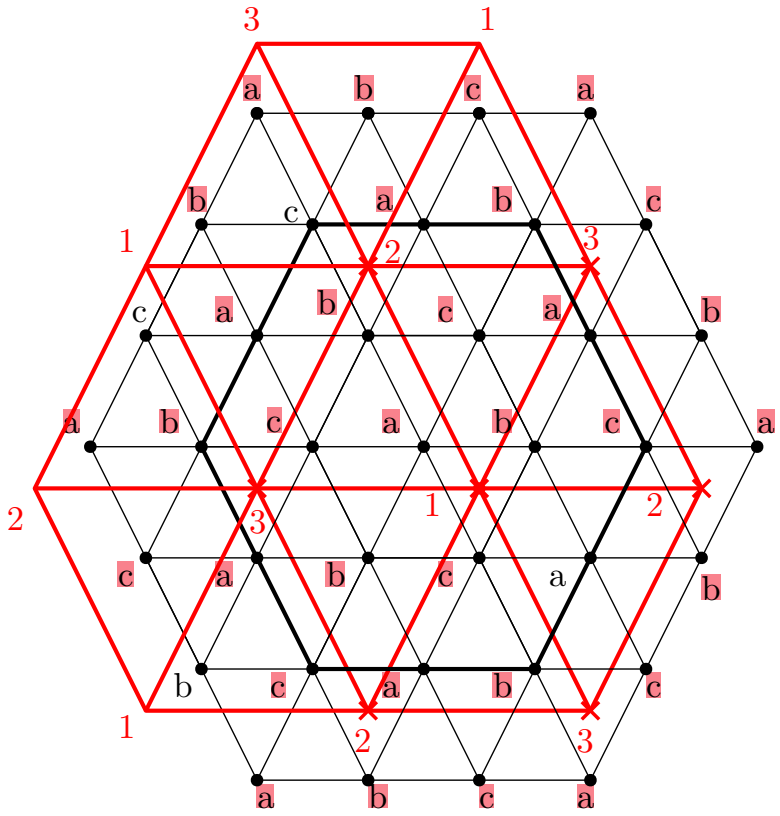

Figure 3.4: Superimposition of L_1 and L_0 with all 3 color classes selected at both refinement levels

We know that every positive integer k can be uniquely expressed in base 4 as

$$k = \sum_{t=0}^{T} d_t \, 4^t, \qquad d_t \in \{0, 1, 2, 3\}. \tag{3.1}$$

From Theorem 3.2, for each refinement level $\mathcal{L}_t$, choose exactly d_t color classes among $\{A, B, C\}$ and place sensors at every vertex of the chosen colors. If $d_t = 0$, no vertices are selected from $\mathcal{L}_t$.

By Theorem 1, each chosen color class on $\mathcal{L}_t$ contributes at least 4^t to the minimum guaranteed coverage. Summing these contributions over all levels yields

$$\text{Guaranteed coverage} \;\geq\; \sum_{t=0}^{T} d_t 4^t \;=\; k,$$

where T is the number of refinement levels.

Computing Finite Refinement Depth T: The number of refinement levels depends

on the required coverage k.

For a given k, we construct refinement levels up to

$$T = \lfloor \log_4 k \rfloor . \tag{3.2}$$

Thus, the deployment uses the collection of different refined lattices $\{L_0, L_1, \ldots, L_T\}$, where lattice L_T represents a triangular lattice structure with vertex spacing $r_0/2^T$. Thus, every integer k is realizable by an appropriate selection of color classes across refinement levels as described below.

Selecting refinement levels and color classes: Given a desired coverage level k:

1. Express k in base 4 as $k = \sum_{t=0}^{T} d_t 4^t$, with $d_t \in \{0, 1, 2, 3\}$.
2. For each t, activate d_t distinct color classes on L_t (e.g., choose A, B, C in order as needed).
3. Place sensors at every vertex of the selected color classes.

It is now evident that the *superimposition* of the selected refinement levels and their corresponding color classes will guarantee the k-coverage everywhere in the interior of the domain.

However, if multiple lattice levels are directly overlaid, some vertices from different refinement levels may coincide. In such cases, multiple sensors would need to be placed at the same location, which is undesirable and leads to inefficient deployment. To support this, in the following section, we propose a centroid-based hierarchical superimposition strategy. Our objective is to provide a superimposition such that the minimum distance δ_{min} between any two sensors is as large as possible.

Chapter 4

CENTROID-BASED HIERARCHICAL SUPERIMPOSITION STRATEGY

For a large k, k-coverage necessitates the superposition of several refinement levels because colocated sensor deployment is explicitly forbidden. However, directly overlaying multiple triangular lattices causes vertex coincidence between different refinement levels, which leads to colocated sensors and inefficient deployment. In this context, we introduce a centroid-based hierarchical superimposition strategy in which coarser lattices are recursively constructed from finer lattices using centroid offsets. The complete process is discussed in detail below.

4.1 Centroid-Based Refinement superimposition

Let L_0 denote the coarsest triangular lattice with side length r_0. For each refinement level $t \geq 1$, the lattice L_t is obtained by subdividing every side of the triangles in L_0 into 2^t equal parts, and hence the resulting lattice spacing becomes

$$a_t = \frac{r_0}{2^t}. \tag{4.1}$$

The finest refinement lattice is constructed first. Coarser lattices are then recursively embedded inside finer lattices using centroid offsets. Specifically, the vertices of lattice L_{t-1} are placed at the centroids of selected equilateral triangles of lattice L_t. Since the

centroid of an equilateral triangle lies strictly inside the triangle and does not coincide with any vertex, this construction guarantees that vertices belonging to different refinement levels remain distinct. The different refinement levels and the color classes can be obtained using Theorem 3.3. The final deployment forms a non-overlapping multi-level hierarchical lattice structure as formally stated in Algorithm 1.

Algorithm 1 Hierarchical Sensor Deployment for Arbitrary k-Coverage

Input: Coverage level k, base lattice spacing r_0

Output: Set S of deployed sensor locations

1. Compute the base-4 coefficients $d_0, d_1, \ldots, d_T$ using Equation 3.1.
2. Initialize $S \leftarrow \emptyset$.
3. Construct the finest refinement lattice L_T with spacing $a_T = r_0/2^T$.
4. For $t = T, T-1, \ldots, 0$:
   (a) If $t < T$, construct lattice L_t by placing its vertices at the centroids of selected triangles of L_{t+1}.
   (b) If $d_t > 0$:
      i. Select d_t distinct color classes from $\{A, B, C\}$.
      ii. Add all vertices of L_t belonging to the selected color classes to S.
5. Return S.

We now illustrate this superimposition strategy by using the following example.

4.2 Illustrative Example

Consider the required coverage $k = 21$. The base-4 decomposition of k is

$$15 = 3 \cdot 4^1 + 3 \cdot 4^0.$$

Hence, refinement levels L_1, and L_0 must all participate in the deployment.

The deployment proceeds as follows:

1. Construct the finest lattice L_1 with spacing $a_2 = \frac{r_0}{2}$. Activate all three color classes on L_1.

2. Construct lattice L_0 by placing its vertices at centroids of selected triangles of L_1. Activate all three color classes on L_0.

Therefore, the final deployment becomes

$$S = L_0 \cup L_1.$$

Thus, the proposed centroid-based hierarchical superimposition realizes exact 15-coverage to the FOI while ensuring that sensors belonging to different refinement levels

are placed at distinct physical locations. The superimposition of L_0 from Fig. 3.2 and L_1 from Fig. 3.3 with all 3 color classes chosen is illustrated in Fig. 3.4.

In the following section, we derive closed-form expressions for the sensor density and sensor spacing δ_{min} achieved for k-coverage under the proposed hierarchical deployment strategy.

Chapter 5

Analysis of Sensor Density and Sensor Spacing

In the following two subsections, we compute the sensor density and sensor spacing for the proposed deployment strategy, respectively.

5.1 Sensor Density Computation

We consider an equilateral triangle of side length r_0 as a unit cell for a triangular lattice. This decision is quite natural because an equilateral triangle is an element that can not be broken down further – a triangular lattice consists of these triangles, which can completely fill the plane through translation and reflection. At refinement level t, the lattice spacing reduces to $a_t = r_0/2^t$, and each base triangle of side length r_0 is subdivided into 4^t smaller equilateral triangles of side length a_t. The total number of lattice vertices $V_\triangle(t)$ inside (and on the boundary of) one base equilateral triangle at refinement level t is given by:

$$V_\triangle(t) = \frac{(2^t+1)(2^t+2)}{2} = \frac{4^t}{2} + \frac{3\cdot 2^t}{2} + 1. \tag{5.1}$$

Thus, asymptotically,

$$V_\triangle(t) \sim \frac{4^t}{2} \quad \text{as } t \to \infty. \tag{5.2}$$

The triangular lattice is three-colorable. The $V_\triangle(t)$ lattice vertices of the base equilateral triangle are distributed equally among the three color classes, as stated in the following lemma.

At refinement level t, each color class contains exactly

$$V_{\triangle}^{(\text{class})}(t) = \frac{V_{\triangle}(t)}{3} = \frac{(2^t+1)(2^t+2)}{6} \tag{5.3}$$

vertices within the base equilateral triangle.

At refinement level t, the base triangle is subdivided into 4^t elementary sub-triangles. Each elementary sub-triangle contains exactly one vertex of each color class. Hence the total vertices is distributed equally per color class.

As d_t color classes are activated at refinement level L_t, the total number of active sensors within the base equilateral triangle is:

$$N_{\triangle}(t) = d_t \cdot \frac{(2^t+1)(2^t+2)}{6}. \tag{5.4}$$

Asymptotically,

$$N_{\triangle}(t) \sim \frac{d_t \cdot 4^t}{6} \quad \text{as } t \to \infty. \tag{5.5}$$

Now total number of activated sensors across all refinement levels $t = 0, 1, \ldots, T$ is given by:

$$N_{\triangle}^{\text{total}} = \sum_{t=0}^{T} d_t \cdot \frac{(2^t+1)(2^t+2)}{6}. \tag{5.6}$$

Asymptotically,

$$N_{\triangle}^{\text{total}} \sim \sum_{t=0}^{T} \frac{d_t \cdot 4^t}{6} = \frac{k}{6} \quad \text{as } t \to \infty. \tag{5.7}$$

The area of the base equilateral triangular unit is:

$$A_{\triangle} = \frac{\sqrt{3}}{4} r_0^2. \tag{5.8}$$

Thus, the sensor density is:

$$\rho(k) = \frac{N_{\triangle}^{\text{total}}}{A_{\triangle}} = \frac{\sum_{t=0}^{T} d_t \cdot \frac{(2^t+1)(2^t+2)}{6}}{\sqrt{3}\, r_0^2/4}. \tag{5.9}$$

Asymptotically,

$$\rho(k) = \frac{N_{\triangle}^{\text{total}}}{A_{\triangle}} = \frac{k/6}{\sqrt{3}\, r_0^2/4} = \frac{2k}{3\sqrt{3}\, r_0^2} \approx \frac{0.3849\, k}{r_0^2}. \tag{5.10}$$

5.2 Sensor Spacing Computation

To compute the minimum sensor spacing δ_{min}, we first derive the intra-level minimum sensor spacing $\delta_{\text{intra}}^{(t)}$, i.e., the miniumum spacing between the sensors belonging to the same refinement level. Since adjacent vertices of the triangular lattice are separated by exactly one lattice edge, the minimum spacing between two sensors belonging to the same refinement level equals the lattice spacing itself. Therefore, from Equation (4.1), the intra-level sensor spacing at refinement level L_t becomes

$$\delta_{\text{intra}}^{(t)} = a_t = \frac{r_0}{2^t}. \tag{5.11}$$

It can be observed that the intra-level spacing decreases geometrically with increasing refinement depth.

We now derive the inter-level minimum sensor spacing $\delta_{\text{inter}}^{(t)}$, i.e., the minimum sensor spacing between the sensors belonging to two consecutive refinement levels. The proposed hierarchical deployment superimposes a lattice L_{t-1} inside a lattice L_t using centroid-based placement. Now consider an equilateral triangle of side length $a_t = \frac{r_0}{2^t}$. The centroid of the triangle is used as the placement location for the corresponding vertex of the coarser lattice L_{t-1}. Additionally, note that for an equilateral triangle of side length a_t, the height is $\frac{\sqrt{3}}{2}a_t$, and the centroid divides the median in the ratio $2:1$. Therefore, the distance from the centroid to any vertex becomes $\frac{2}{3} \cdot \frac{\sqrt{3}}{2} a_t = \frac{a_t}{\sqrt{3}}$. Hence, the minimum inter-level spacing between sensors belonging to lattices L_t and L_{t-1} is

$$\delta_{\text{inter}}^{(t)} = \frac{a_t}{\sqrt{3}} = \frac{r_0}{\sqrt{3}\, 2^t}. \tag{5.12}$$

It is evident from Equations (5.11) and (5.12), that

$$\frac{r_0}{\sqrt{3}\, 2^t} < \frac{r_0}{2^t} \implies \delta_{\text{inter}}^{(t)} < \delta_{\text{intra}}^{(t)}. \tag{5.13}$$

So the minimum sensor spacing is given by:

$$\delta_{min}^{(t)} = \min\{\delta_{\text{intra}}^{(t)}, \delta_{\text{inter}}^{(t)}\} = \delta_{\text{inter}}^{(t)} = \frac{r_0}{\sqrt{3}\, 2^t}. \tag{5.14}$$

From Equation (5.14), we observe that $\delta_{min}^{(t)}$ decreases monotonically as the refinement becomes finer. Hence, the smallest spacing occurs at the finest active refinement level T. Hence the global minimum sensor spacing $\delta_{\min}$ between any two deployed sensors becomes

$$\delta_{\min} = \delta_{\text{inter}}^{(T)} = \frac{r_0}{\sqrt{3}\,2^T}. \tag{5.15}$$

We now relate the refinement depth T to the required coverage level k. Since L_T is the finest active refinement level, we must have $d_T \neq 0$. Therefore, from (3.2), we have

$$4^T \leq k < 4^{T+1}. \tag{5.16}$$

After trivial algebraic manipulations, Equation (5.16) results in

$$2^T \leq \sqrt{k} < 2^{T+1} \implies 2^T = \Theta(\sqrt{k}). \tag{5.17}$$

Therefore, using Equation (5.17) in Equation (5.15), we obtain

$$\delta_{\min} = \frac{r_0}{\sqrt{3}\,2^T} = \Theta\left(\frac{r_0}{\sqrt{k}}\right). \tag{5.18}$$

Hence, from (5.18), we can conclude the following remark. The minimum sensor spacing decreases proportionally to $1/\sqrt{k}$ as the required coverage level increases.

The density analysis presented above provides the number of sensors required per base equilateral triangle. Although such density expressions are useful for large-scale performance evaluation, they do not provide the exact number of sensors required for a finite deployment region. The reason can be explained as follows. Note that any two adjacent base triangles share common sensors. As lattice spacing decreases, i.e., at finer refinement levels, these common sensors increases. So if we compute the number of sensors for a finite area using density expressions given by Equations 5.9, it will hugely overcount the number of sensors.

In practical WSN deployment, the FOI is finite and sensors can only be placed at discrete lattice vertices. Consequently, boundary effects, vertex sharing, and the discrete nature of the hierarchical refinement process introduce deviations from the exact required number of sensors. Therefore, an exact finite-domain sensor-count expression is required to determine the precise number of sensors needed to achieve a desired k-coverage within a given finite FOI $H(x, z, y)$.

The results derived in the following section complement the asymptotic density analysis by providing an exact closed-form expression for the number of deployed sensors in a finite domain.

Chapter 6

Exact Number of Sensors for k-Coverage in a Finite FOI $H(x, z, y)$

As we have assumed, FOI is a irregular hexagon H(x,z,y), constructed over the base triangular lattice L_0, as shown in Fig 3.1. The hexagon has two vertical sides of lengths y and z (where $y \geq z$), and a top side is of length x. Since the hexagon is aligned with the base lattice L_0, its side lengths can be expressed as integer multiples of the lattice spacing r_0, i.e.,

$$x = c\,r_0, \quad z = e\,r_0, \quad y = d\,r_0$$

for some positive integers c, e, d. Here, R denotes the sensing radius of an individual sensor and is measured in units of length. The side length of the base triangular lattice is chosen as $r_0 = R$. The quantities x, z, and y denote the physical side lengths of the deployment region and therefore have the same units as R. The corresponding lattice coordinates c, e, and d represent the number of lattice edges along the three principal directions of the hexagonal region and are dimensionless integers.

6.1 Relationship Between Physical Dimensions and Lattice Coordinates

The quantities c, e, d represent lattice-coordinate side lengths, i.e., the number of lattice edges along the three principal directions of the triangular lattice. For a physical

deployment region having side lengths x, z, y, the corresponding lattice coordinates are

$$c = \left\lceil \frac{x}{r_0} \right\rceil, \qquad e = \left\lceil \frac{z}{r_0} \right\rceil. \qquad d = \left\lceil \frac{y}{r_0} \right\rceil,$$

Since $r_0 = R$, the lattice coordinates depend on the sensing radius. Consequently, increasing the sensing radius decreases the number of lattice edges required to cover a fixed physical region, thereby reducing the total number of deployed sensors. The exact sensor-count expressions are derived in lattice coordinates (c, e, d), while the sensing radius R influences the deployment through the mapping between physical dimensions and lattice coordinates.

6.2 Geometric Model and Refinement Scheme

The hexagon region is tessellated using equilateral triangles of side length r_0, forming the base triangular lattice. At refinement level t, each side of the triangles is subdivided into 2^t equal parts, resulting in a finer lattice L_t with side length $s = \frac{r_0}{2^t}$. Note that this refinement preserves the overall geometry of the hexagon while increasing the density of lattice vertices. Therefore, the side lengths of the hexagon, measured in terms of the refined lattice L_t, become

$$A = c \cdot 2^t, \quad C = e \cdot 2^t, \quad B = d \cdot 2^t,$$

Furthermore, the refined side lengths are related to the physical dimensions by

$$A = \frac{2^t x}{r_0}, \quad C = \frac{2^t z}{r_0}, \quad B = \frac{2^t y}{r_0}.$$

where A, C, B denote the number of segments along the corresponding sides of the hexagon. Thus, the physical dimensions of the hexagon remain unchanged, but the number of lattice vertices increases with refinement. In the full-coverage scenario, each vertex of the refined lattice represents a potential sensor location.

6.3 Total Number of Sensors inside $H(x, z, y)$

Starting from the top side of the hexagon and working downward, the lattice vertices are counted row by row to establish the total number of sensors needed.

6.3.1 Top Half (Increasing Rows)

There are $(A + 1)$ vertices in the first (topmost) row. Up until the number of rows equals C, each consecutive row gains one vertex demonstrated in Fig 3.1. As a result,

the upper (growing) portion's total vertex count is:

$$N_{\text{top}} = \sum_{i=0}^{C-1} (A+1+i) = C(A+1) + \frac{C(C-1)}{2}. \tag{6.1}$$

The hexagon's lower half contributes an equal number of vertices because it is symmetric. Therefore, from Equation (6.1), we obtain that the total vertices for both ramps is

$$N_{\text{ramp}} = 2N_{\text{top}} = 2C(A+1) + C(C-1). \tag{6.2}$$

6.3.2 Middle Region (Constant Width Rows)

The maximum horizontal span of the hexagon is represented by a series of middle rows of constant width that are situated between the two ramps shown in 3.1. In every middle row, there are:

$$N_{\text{row}} = A + C + 1 \tag{6.3}$$

vertices, and the number of such constant-width rows is

$$N_{\text{rows}} = (B - C + 1), \tag{6.4}$$

Therefore, we obtain the total number of vertices in the middle section's as

$$N_{\text{mid}} = (A + C + 1) * (B - C + 1). \tag{6.5}$$

6.3.3 Total Number of Vertices

The contributions from the ramp regions and the middle region are added to determine the total number of vertices in the irregular hexagonal region:

$$\begin{aligned} N_{\text{total}} = N_{\text{ramp}} + N_{\text{mid}} = [\,2C(A+1) + C(C-1)\,] \\ +[\,(A+C+1)(B-C+1)\,]. \end{aligned} \tag{6.6}$$

The number of sensors as a function of coverage k and side lengths (x, y, z) can be obtained by substituting A, B, and C:

$$N_t^{(\text{int})} = 4^t(cd + ce + de) + 2^t(c + d + e) + 1 \tag{6.7}$$

This expression gives the *exact number of lattice vertices* for obtaining full vertex coverage in an irregular hexagon after k stages of subdivision.

Suppose $d_t \in \{0, 1, 2, 3\}$ color classes are activated at refinement level t. Then the total number of interior deployment sensors becomes

$$N_{\text{int}} = \sum_{t=0}^{T} d_t[4^t(cd + ce + de) + 2^t(c + d + e) + 1]. \tag{6.8}$$

6.4 Total Number of Sensors outside $H(x, z, y)$

Previous subsection computes the required number of sensors inside a hexagonal region $H(x, z, y)$. However, for finite regions, additional lattice sensors may be required outside the boundary for providing k-coverage to the region near the edge of $H(x, z, y)$.

At the refinement level t, compared to the base lattice, this introduces $2^t - 1$ new subdivision points along each side of the hexagon. Since the hexagon has six sides, the number of additional refinement-induced boundary-support sensors required at level t becomes

$$N_t^{\text{bdry}} = 6(2^t - 1) \tag{6.9}$$

which satisfies the consistency condition $N_0^{\text{bdry}} = 0$.

Therefore, from (3.1) and (6.9), we obtain the total number of sensors as

$$N_{\text{bdry}} = \sum_{t=0}^{T} d_t\, 6(2^t - 1). \tag{6.10}$$

6.5 Exact Total Sensor Count

Combining both interior and boundary-support sensors, the exact total number of deployed sensors required for finite hexagonal domain coverage is

$$N_{\text{total}} = N_{\text{int}} + N_{\text{bdry}}. \tag{6.11}$$

Substituting the corresponding expressions,

$$N_{\text{total}} = \sum_{t=0}^{T} d_t/3[4^t(cd + ce + de) + 2^t(c + d + e) + 1 + 6(2^t - 1)] \tag{6.12}$$

Simplifying,

$$N_{\text{total}} = \sum_{t=0}^{T} d_t/3[4^t(cd + ce + de) + 2^t(c + d + e + 6) - 5] \tag{6.13}$$

Chapter 7

Comparative Analysis with Existing Deployment Strategies

In this section, we compare the proposed hierarchical triangular refinement deployment with three existing deterministic k-coverage deployment strategies:

1. Irregular hexagonal (IRH) edge-overlap deployment [3],
2. Irregular hexagonal (IRH) inner-diamond deployment [7], and
3. Square-band deployment [8].

The authors of [3] and [7] take into consideration the triangular lattice with fixed side r/n, where r is the sensing radius and $n > 1$. In [3], the authors consider a irregular hexagon as a block and deploy k sensors on a selected edge of that block to provide k-coverage of it. They then tile the entire lattice using that block. In [7] authors first consider a diamond shape area and place k sensors inside that diamond area which provides k-coverage to a common irregular hexagon area. They then use that irregular hexagon to tile the entire lattice. The square tessellation of the field of interest and sensors with diverse sensing radii are taken into consideration by the authors in [8] in place of the triangular lattice. In order to offer k-coverage to a diamond-shaped block inside a square with side r, they first position some sensors with lower radius inside the square and some extra sensors with radius larger than the lower radius. The diamond-shaped block is then used to tile the area of interest.

The comparison is performed using two important geometric performance metrics: 1) asymptotic sensor density and 2) minimum sensor spacing.

7.1 Comparison with IRH Edge-Overlap Deployment

In this subsection, we will compare sensor density and sensor spacing obtained by our approach with that obtained in [3].

7.1.1 Sensor Density Comparison

The IRH-based deployment [3] constructs irregular hexagonal regions by placing k sensors along the common edge shared by adjacent regular hexagons. For the generalized IRH(r/n) construction, the deployed sensor density is given by

$$\psi_{\text{IRH}}(r,k,n) = \frac{4nk}{\sqrt{3}(6n-4)r^2}. \tag{7.1}$$

For large n, $6n-4 \sim 6n$. Therefore, Equation (7.1) can be written as

$$\psi_{\text{IRH}}(r,k,n) \sim \frac{2k}{3\sqrt{3}\,r^2}. \tag{7.2}$$

Now from Equations (5.10) and (7.2), we obtain the density ratio as

$$\frac{\rho_{\text{ours}}(k)}{\psi_{\text{IRH}}(r,k,n)} = \frac{\frac{2k}{3\sqrt{3}\,r^2}}{\frac{2k}{3\sqrt{3}\,r^2}} = 1. \tag{7.3}$$

Therefore, the proposed deployment achieves the same asymptotic density with respect to our approach density than IRH edge-overlap deployment.

7.1.2 Sensor Spacing Comparison

In the IRH-based deployment [3], k sensors are concentrated along a common edge of length approximately $\frac{r}{n}$. Therefore, the minimum spacing between adjacent sensors approximately becomes $\delta_{\text{IRH}} \approx \dfrac{r/n}{k-1}$.

For large k, $k-1 \sim k$. Hence,

$$\delta_{\text{IRH}} = \Theta\left(\frac{r}{nk}\right). \tag{7.4}$$

Therefore, from (5.18) and (7.4), we obtain

$$\frac{\delta_{\text{min}}^{\text{ours}}}{\delta_{\text{IRH}}} = \Theta\left(\frac{r/\sqrt{k}}{r/(nk)}\right) = \Theta(n\sqrt{k}). \tag{7.5}$$

Hence, the proposed deployment preserves significantly larger sensor spacing than IRH-based deployment.

7.2 Comparison with IRH Inner-Diamond Deployment

In this subsection, we will compare sensor density and sensor spacing obtained by our approach with that obtained in [7].

7.2.1 Sensor Density Comparison

The IRH inner-diamond deployment [7] achieves k-coverage by placing sensors inside compact inner-diamond regions associated with irregular hexagonal tiles. The deployed sensor density derived in the corresponding work is

$$\lambda_{\text{ID}}(k, r_s, n) = \frac{k}{\left(\pi + \frac{(3n^2-6n+2)\sqrt{3}}{4n^2} - \frac{\sqrt{4n^2-1}}{n^2} - 4\sin^{-1}\left(\frac{1}{2n}\right)\right) r_s^2}. \tag{7.6}$$

Therefore, after a few algebraic computations, from Equation (7.6) for $n \to \infty$, we obtain

$$\lambda_{\text{ID}}(k, r_s, n) = \frac{k}{\left(\pi + \frac{3\sqrt{3}}{4}\right) r_s^2} \approx 0.2252 \frac{k}{r_s^2}. \tag{7.7}$$

Finally, from Equations (5.10) and (7.7), we obtain

$$\lambda_{\text{ID}}(k, r_s, n) < \frac{0.3849\, k}{r_0^2} = \rho_{\text{ours}}(k). \tag{7.8}$$

It is evident that the inner-diamond deployment achieves lower asymptotic sensor density than the proposed deployment.

7.2.2 Sensor Spacing Comparison

In the inner-diamond deployment, all k sensors are placed inside a compact inner-diamond region whose characteristic diameter scales as $\Theta\left(\frac{r_s}{n}\right)$. Since k sensors are packed inside this shrinking region, the minimum sensor spacing approximately scales as

$$\delta_{\text{ID}} = \Theta\left(\frac{r_s}{n\sqrt{k}}\right). \tag{7.9}$$

Moreover, from Equations (5.18) and (7.9), we obtain the sensor the spacing ratio as

$$\frac{\delta_{\text{min}}^{\text{ours}}}{\delta_{\text{ID}}} = \Theta\left(\frac{r_s/\sqrt{k}}{r_s/(n\sqrt{k})}\right) = \Theta(n). \tag{7.10}$$

Therefore, the proposed deployment preserves significantly larger sensor spacing than

the inner-diamond deployment as the tessellation refinement parameter n increases. It is important to observe that the asymptotic density Improvement of the inner-diamond deployment is achieved by increasing the tessellation refinement parameter n. As $n \to \infty$, the characteristic diameter of the inner-diamond region satisfies $\Theta\left(\frac{r_s}{n}\right) \to 0$. Consequently, the minimum sensor spacing also decreases toward zero, i.e., $\delta_{\text{ID}} = \Theta\left(\frac{r_s}{n\sqrt{k}}\right) \to 0$.

Thus, the asymptotic density improvement is obtained at the cost of increasingly severe sensor clustering. In the limiting case, $n \to \infty$, multiple sensors become arbitrarily close to each other in the two-dimensional deployment plane, which is physically impractical for real wireless sensor network deployments. In contrast, the proposed hierarchical triangular refinement deployment does not rely on collapsing deployment regions. Its minimum sensor spacing remains explicitly bounded by $\delta_{\min}^{\text{ours}} = \Theta\left(\frac{r_0}{\sqrt{k}}\right)$, independent of any additional tessellation refinement parameter. Hence, the proposed deployment preserves non-zero geometric separation between deployed sensors while maintaining deterministic multilevel k-coverage.

7.3 Comparison with Square-Band Deployment

In this subsection, we will compare sensor density and sensor spacing obtained by our approach with that obtained in [8].

7.3.1 Sensor Density Comparison

The heterogeneous square-band deployment [8] partitions the sensing field into multiple square bands using heterogeneous sensors with minimum and maximum sensing radii $r_s^{\min}$ and $r_s^{\max}$. The asymptotic deployed density derived in that work is

$$\lambda_{\text{HSB}} = \Theta\left(\frac{2k}{(r_s^{\min} + r_s^{\max})^2}\right). \tag{7.11}$$

For $r_0 = r_s^{\min}$, from Equations (5.10) and (7.11), we obtain the density as

$$\frac{\rho_{\text{ours}}(k)}{\lambda_{\text{HSB}}} = \frac{(r_s^{\min} + r_s^{\max})^2}{3\sqrt{3}\,(r_s^{\min})^2} = \frac{\left(1 + \frac{r_s^{\max}}{r_s^{\min}}\right)^2}{3\sqrt{3}}. \tag{7.12}$$

Therefore, the proposed deployment achieves lower density whenever $\frac{r_s^{\max}}{r_s^{\min}} < 1.279$. For $\frac{r_s^{\max}}{r_s^{\min}} > 1.279$, the heterogeneous deployment may achieve lower density due to the

availability of significantly larger sensing-radius sensors capable of covering substantially larger regions. Thus, the density improvement in the heterogeneous square-band deployment originates primarily from sensor heterogeneity rather than purely geometric deployment efficiency.

7.3.2 Sensor Spacing Comparison

In the heterogeneous square-band deployment, sensors are distributed within square tiles of side length proportional to $r_s^{\min}$. Since each tile contains k sensors, the minimum spacing approximately scales as

$$\delta_{\mathrm{HSB}} = \Theta\left(\frac{r_s^{\min}}{\sqrt{k}}\right). \tag{7.13}$$

Now, using $r_0 = r_s^{\min}$, from (5.18) and (7.13), we obtain

$$\delta_{\min}^{\mathrm{ours}} = \Theta\left(\delta_{\mathrm{HSB}}\right). \tag{7.14}$$

Therefore, both approaches exhibit the same asymptotic spacing order.

7.4 Practical Advantages of the Proposed Deployment

Beyond asymptotic density and spacing analysis, the proposed hierarchical triangular refinement deployment provides several important practical advantages arising from its distributed multilevel geometric structure.

7.4.1 Robustness Against Localized Failures

Many existing deterministic k-coverage deployment strategies achieve density improvement through strong local sensor clustering. This can drastically reduce the local coverage multiplicity.

7.4.2 Balanced Density–Spacing Tradeoff

Several existing approaches achieve low asymptotic density by allowing the minimum sensor spacing to collapse toward zero. Thus, density improvement is obtained at the cost of severe local sensor clustering. The proposed deployment, however, maintains the minimum sensor spacing while simultaneously achieving competitive asymptotic sensor density.

3

7.4.3 Gradual Coverage Degradation Outside the Region of Interest

In the proposed deployment, the region of interest receives deterministic full k-coverage through hierarchical superposition of multiple refinement levels. However, due to the distributed geometric structure of the lattices, the coverage multiplicity outside the target region decreases gradually. In contrast, highly clustered deployment strategies often produce abrupt coverage discontinuities near deployment boundaries due to strong local overlap concentration.

Chapter 8

Numerical Results

This section focuses on evaluating the performance of the proposed hierarchical triangular refinement deployment algorithm against past k-coverage deployments using numerical techniques. The objective of this analysis is to study the features of the proposed algorithm concerning sensor density, number of sensors required, and minimum spacing between them. Homogeneous sensor networks with sensing radius ($R = r_0$) are assumed unless stated otherwise. The network coverage area is taken as an irregular hexagon $H(x, z, y)$ defined on a base triangle lattice. The analytical results developed in Section 5 to evaluate the necessary performance parameters. In other words, the proposed network topology is analyzed against IRH edge-overlap deployment [3] and IRH inner-diamond deployment [7], as well as a heterogeneous square-band deployment [8].

8.1 Simulation Setup

The numerical calculations shown in this section have been performed based on the analytical expressions provided in Sections 5 – 6. Unless specified otherwise, all cases considered involve sensors which have the same radius of sensing, i.e., $R = r_0$. The sensing zone is defined by an irregular hexagon $H(x, z, y)$ on the base triangular lattice network. The density and spacing formulae calculations for IRH edge-overlap deployment, IRH inner diamond deployment, and heterogeneous square-band deployment are also included for reference.

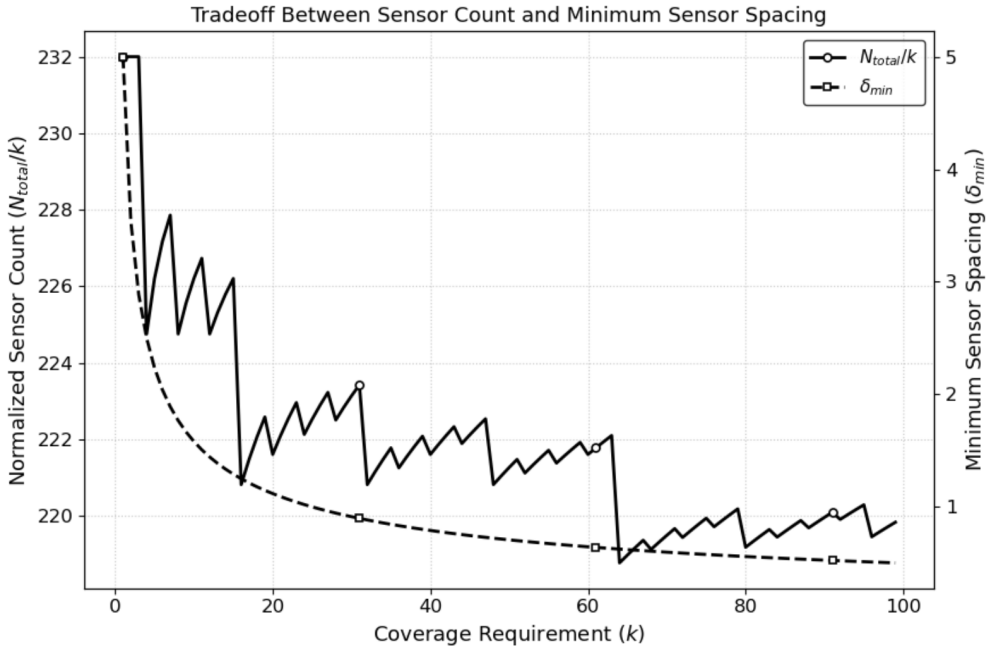

Figure 8.1: Tradeoff Between Sensor Count and Minimum Sensor Spacing Under Increasing Coverage Requirements

8.2 Effect of Coverage Requirement on Sensor Count and Minimum Sensor Spacing

Fig. 8.1 shows the impact of the required coverage level k on the normalized sensor count, defined as the ratio of number of sensors to k, and the minimum sensor spacing achieved by the proposed hierarchical deployment strategy. The deployment region is fixed at $H(15, 10, 20)$ and the sensing radius is fixed at $r_0 = 5\ m$.

As the coverage value k increases, the normalized sensor count decreases like a staircase function and becomes approximately constant after certain coverage level. This comes directly from the analytical sensor-count expression we have derived in Section 5, that shows the number of deployed sensors grows approximately linearly with the required coverage level k. Consequently, the ratio N_{total}/k approaches a nearly constant value for large coverage value of k.

The minimum sensor spacing decreases as more refinement levels become necessary. From Equation (5.18), we get δ_{min} is proportional to $\frac{1}{\sqrt{k}}$. Note that this sensor spacing is computed by assuming that sensors are placed at all the vertices at the corresponding refinement levels. Thus the actual sensor spacing will be little more when we do need not to activate all sensors.

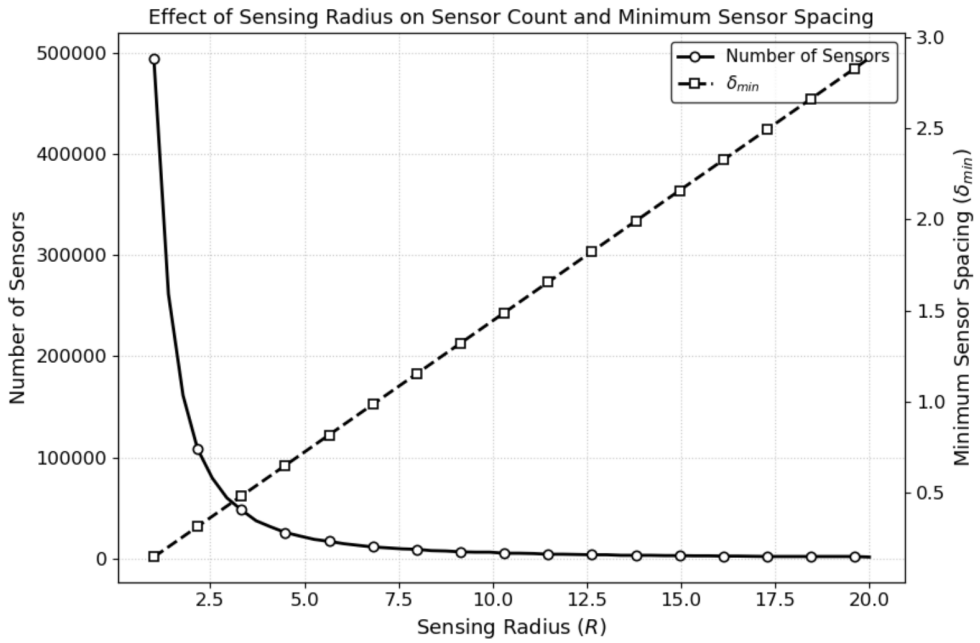

Figure 8.2: Effect of Sensing Radius on Sensor Count and Minimum Sensor Spacing

8.3 Effect of Sensing Radius on Sensor Count and Minimum Sensor Spacing

Fig. 8.2 shows the effect of the sensing radius R on the number of deployed sensors and the minimum sensor spacing for a fixed coverage requirement of $k = 50$. The deployment region is fixed at $H(100, 80, 120)$.

As we increase the radius of sensor, the number of sensors needed reduces rapidly. This was expected since a higher sensing radius means that the sensor can cover a larger physical area, thus requiring fewer number of sensors to meet the coverage requirement.

In contrast, the minimum sensor spacing increases linearly with the sensing radius. This is because, it is evident from Equation (5.18), that spacing is directly proportional to the sensing radius when the coverage level is fixed.

8.4 Effect of Deployment Region Size

Fig. 8.3 shows the relationship for the number of deployed sensors and the minimum sensor spacing with the size of the deployment region increases. In this experiment, the coverage requirement is fixed at $k = 50$ and the sensing radius is fixed at $r_0 = 10$, and the hexagon region $H(l, l, l)$ assumed regular $x = y = z = l$ and l is varying on X axis.

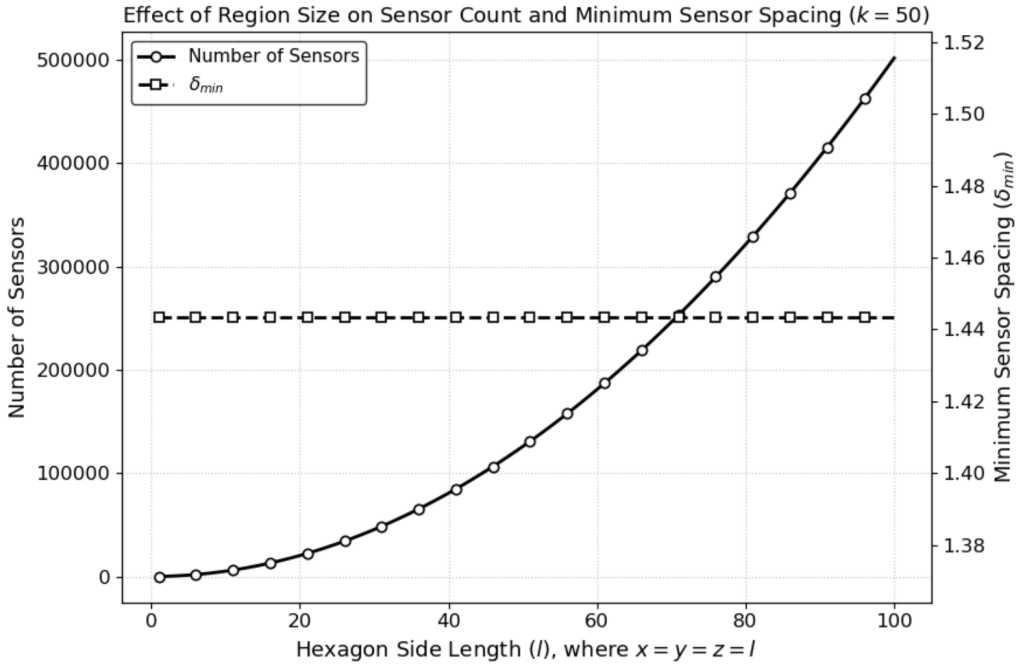

Figure 8.3: Effect of Region Size on Sensor Count and Minimum Sensor Spacing (k=k)

28

As the area of hexagonal region grows proportionally to l^2, thus the number of deployed sensors increases rapidly. The required number of sensors also exhibits approximately quadratic growth. This behavior directly comes from the closed-form equation that we have derived for sensor-count in Equation 6.13, where the dominant term is proportional to $(xy + yz + zx)$.

And the other side, the minimum sensor spacing remains same throughout the experiment. This occurs because the spacing expression (Equation 5.18) is dependent only on the sensing radius for fixed k.

8.5 Comparison of Asymptotic Sensor Density

In Fig. 8.5, it compares the asymptotic sensor density of the proposed hierarchical deployment strategy with three existing k-coverage deployment approaches, namely IRH edge-overlap [3] deployment, IRH inner-diamond [7] deployment, and the heterogeneous square-band [8] deployment.

As expected, the sensor density of all deployment strategies increases linearly with the required coverage level k. This directly follows the corresponding density expressions, all of which are proportional to k.

Among the existing approaches, the IRH edge-overlap [3] deployment has the highest

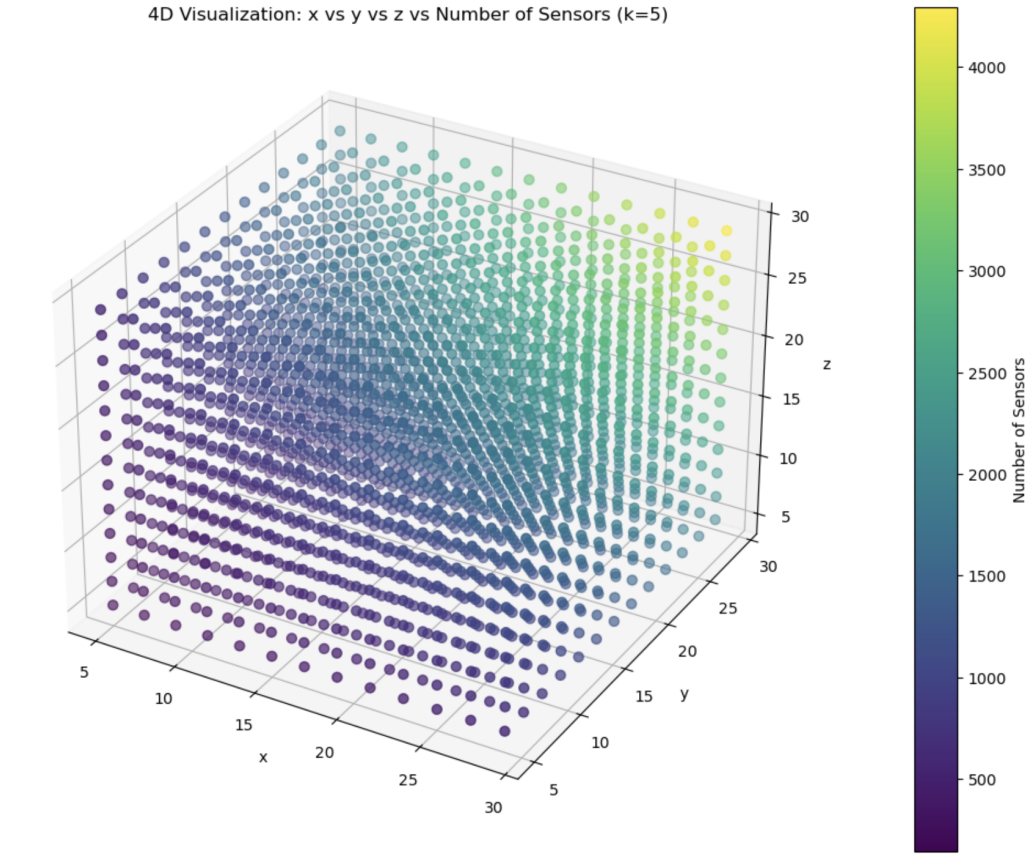

Figure 8.4: 4D Visualization: x vs y vs z vs Number of Sensors (k=5)

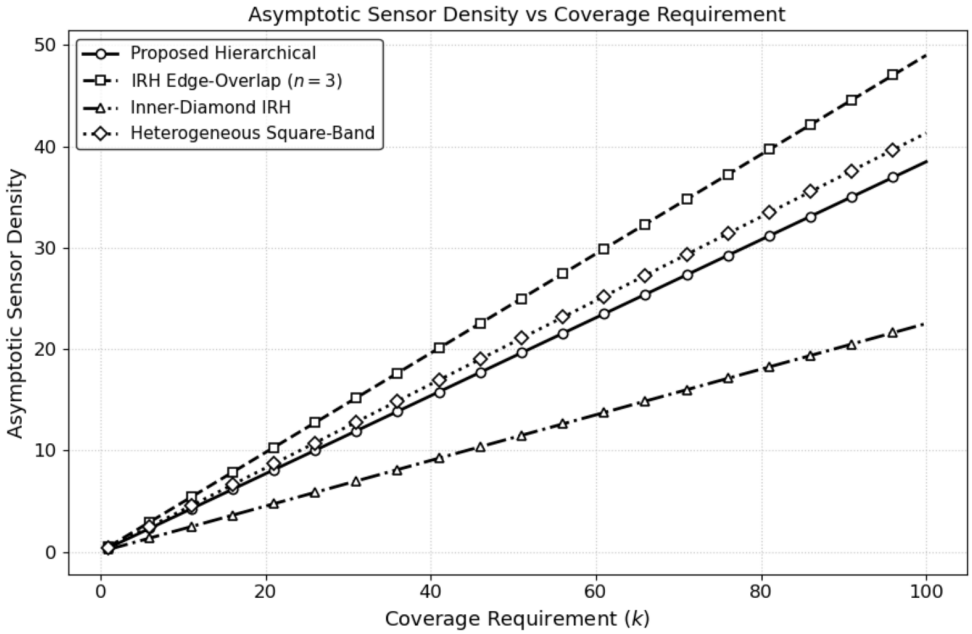

Figure 8.5: Asymptotic Sensor Density vs Coverage Requirement

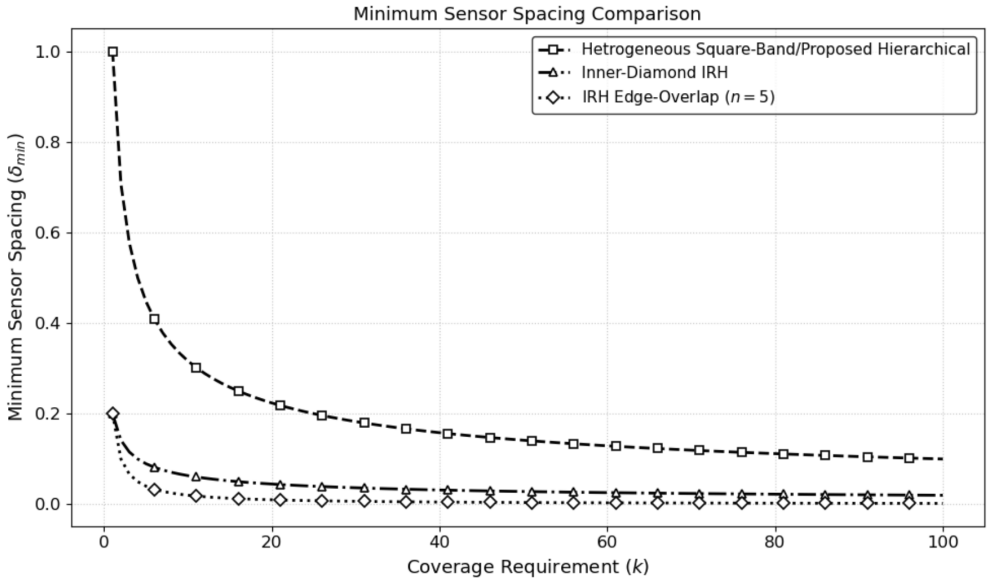

Figure 8.6: Minimum Sensor Spacing vs. Coverage Requirement

density. This behavior comes from the theoretical result derived in Section 7, where the density scales proportionally to the refinement parameter n. For this simulation, we have considered the same value of $n = 3$ as considered in [3]. It is evident that this strategy requires substantially more sensors than the proposed strategy.

The proposed hierarchical deployment method achieves lower density than the heterogeneous square-band deployment while it maintains the same deterministic coverage guarantees. This reduction comes from the hierarchical refinement method and using efficiently color classes across multiple refinement levels. The IRH inner-diamond [7] deployment method achieves the lowest asymptotic density among the all methods. However, as we discussed in Section 7, this density advantage is obtained at the cost of severely reducing sensor spacing.

Overall, the simulation results concludes the similar behavior obtained from the asymptotic density expressions derived earlier. It demonstrate that the proposed deployment strategy creates a balance between deployment density and geometric sensor spacing, by avoiding the heavy clustering associated with past several existing approaches.

8.6 Comparison of Minimum Sensor Spacing

Fig. 8.6 compares the minimum sensor spacing achieved by the proposed deployment with the considered three existing approaches. As expected, sensor spacing decreases as we increase coverage k value for all approaches. As evident from the derived expression (Equation (5.18)), in the proposed deployment strategy, the spacing decreases relatively

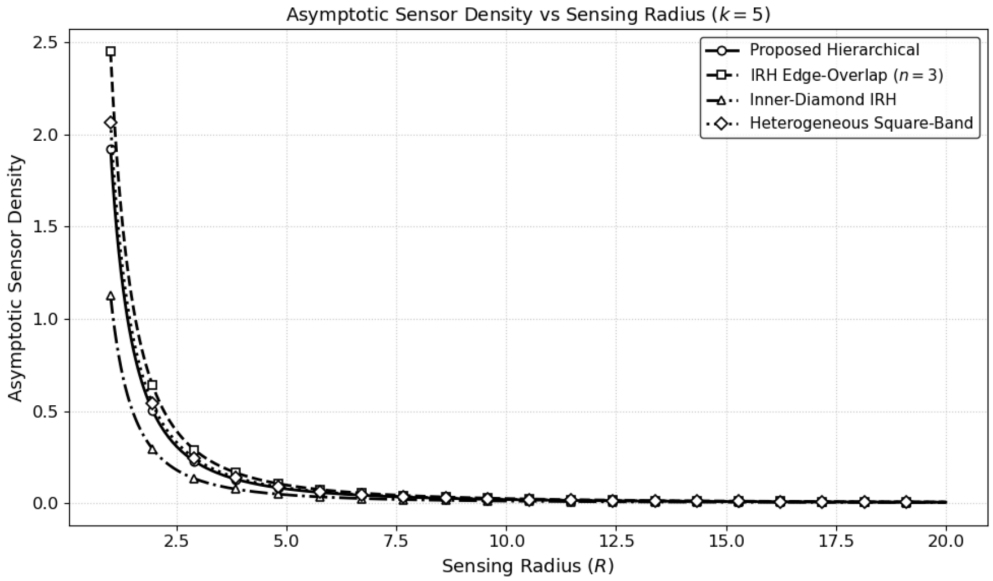

Figure 8.7: Sensor Density vs. Sensing Radius

slowly with increasing coverage. The heterogeneous square-band [8] deployment and the proposed deployment strategy follows a similar asymptotic trend (hence they are plotted as a single curve), where the spacing decreases relatively slowly with increasing coverage. While other side, the inner-diamond [7] deployment gives significantly smaller spacing due to the concentration of sensors inside compact deployment regions and the IRH edge-overlap [3] deployment shows the most rapid spacing degradation, with spacing decreasing approximately as $1/(nk)$.

8.7 Effect of Sensing Radius on Sensor Density

Fig. 8.7 compares the asymptotic sensor density of the considered deployment strategies as a function of the sensing radius R for a fixed coverage requirement of $k = 5$. As we expect, the sensor density decreases rapidly as the sensing radius increases. This behavior directly follows from the density expressions, in which all of them are inversely proportional to R^2. This is quite intuitive as a larger sensing radius allows each sensor to cover a larger area, thus causing in reduction of the number of sensors required per unit area. It is evident that IRH inner-diamond performs best and IRH edge-overlap performs worst and the proposed and heterogeneous square-band perform similarly and lies between them. Note that the superior performance of IRH inner-diamond comes at the cost of sensor spacing. Overall, the results confirm the theoretical density analysis and demonstrate that increasing the sensing radius significantly reduces deployment density for all considered strategies.

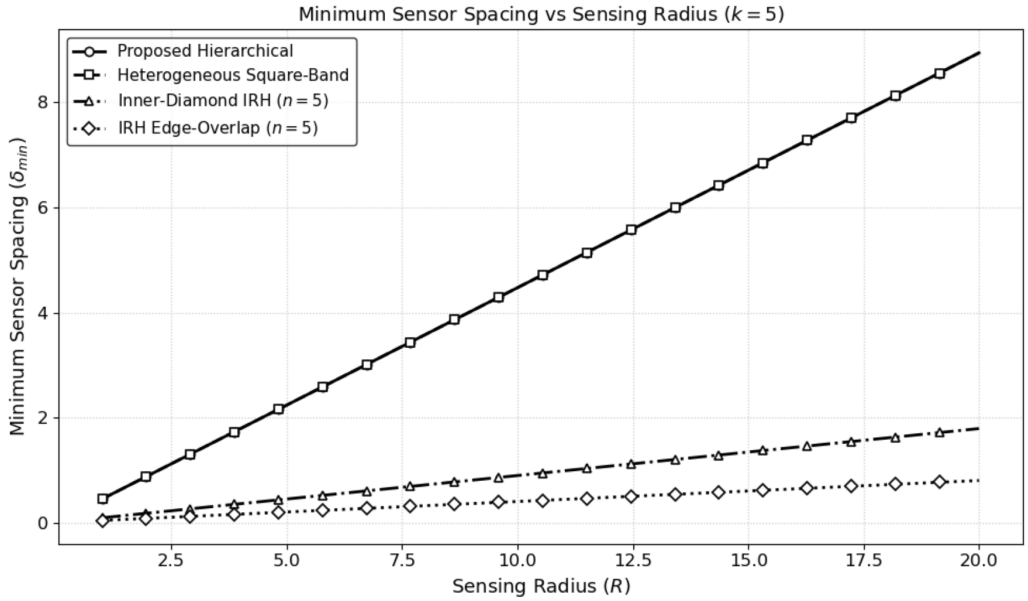

Figure 8.8: Minimum Sensor Spacing vs. Sensing Radius

8.8 Effect of Sensing Radius on Minimum Sensor Spacing

Fig. 8.8 demonstrates the minimum sensor spacing achieved by all the considered deployment strategies as the sensing radius R increases. For all deployment strategies, as we increase the sensor radius the minimum sensor spacing increases linearly. This behavior is expected since larger sensing radius allows neighboring sensors to have a larger separation between them with taking care of required coverage guarantee. The proposed hierarchical deployment and the heterogeneous square-band [8] deployment shows identical asymptotic spacing behavior, which is resulting into overlapping curves. Both approaches maintain spacing proportional to $R/\sqrt{k}$. While other side, the inner-diamond [3] deployment achieves smaller spacing due to the concentration of sensors within on edge.

8.9 Comparison of Sensor Count with Deployment Region Size

Fig. 8.9 compares the number of deployed sensors required by different deployment strategies as the deployment region size increases. In this experiment, the coverage requirement is fixed at $k = 10$, the sensing radius is fixed at $R = 5$, and the deployment region is parameterized by $x = y = z = l$. The number of required sensors increases pretty equally for all deployment strategies as the deployment region grows in size, with the exception of heterogeneous square-band, where the number of sensors becomes

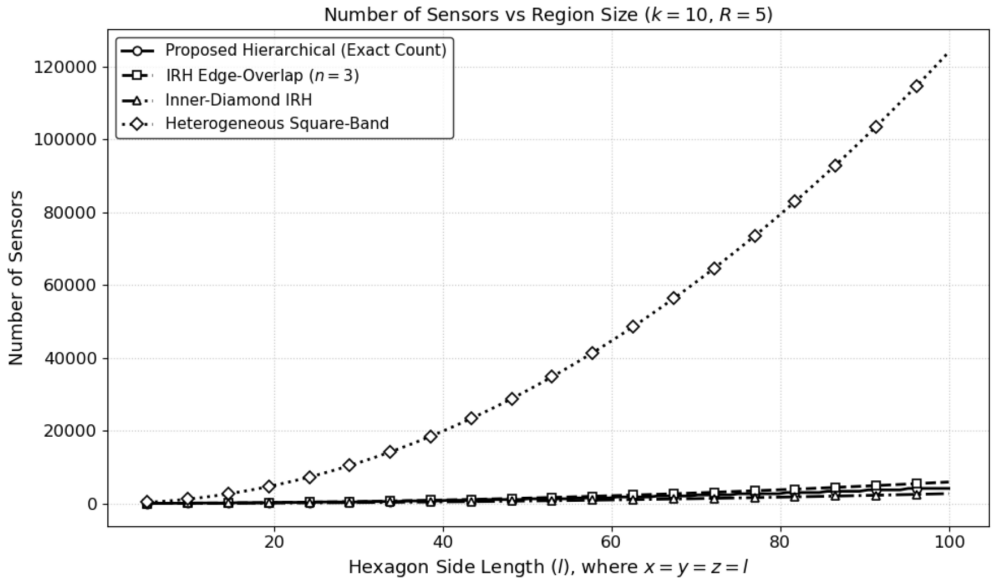

Figure 8.9: Number of Sensors vs Region Size

enormous in comparison to other deployment methods.

Note that heterogeneous square-band performs worst as we have considered ratio of maximum sensing radius r_{max} and minimum sensing radius r_{min} as 1.2. If we increase this ration this approach may perform better. Even though the other three methods perform similarly in terms of the number of sensors needed, the suggested solution performs significantly better in terms of sensor spacing.

Chapter 9

Conclusion

In this work, we proposed a hierarchical triangular lattice-based sensor deployment strategy that organizes sensor locations across different refinement levels and guarantees coverage of every point in the sensing domain by at least k sensors. We derived analytical closed-form expressions for the exact number of sensors and minimum sensor spacing required to ensure k-coverage. Analytical comparison with existing IRH edge-overlap, IRH inner-diamond and square-band based deployment strategies shows that the proposed method either reduces the required number of sensors or increases minimum sensor spacing while maintaining similar coverage guarantees. The derived analytical expressions are also validated through extensive simulations. The suggested framework offers an effective and scalable method for deploying sensors in large-scale wireless sensing systems. Here we have considered the FOI as an irregular hexagon and in future we would like to study arbitrary FOI.

Bibliography

[1] Ericsson Mobility Report. [Online]. Available: https://www.ericsson.com/en/reports-and-papers/mobility-report/reports. Nov. 2025.

[2] I. F. Akyildiz et al. "Wireless sensor networks: a survey". In: *Comput. networks* 38.4 (2002), pp. 393–422.

[3] H. M. Ammari. "A computational geometry-based approach for planar k-coverage in wireless sensor networks". In: *ACM Trans. Sens. Netw.* 19.2 (Feb. 2023), pp. 1–42.

[4] H. M. Ammari. "Investigating the Energy Sink-Hole Problem in Connected k-Covered Wireless Sensor Networks". In: *IEEE Trans. Comput.* 63.11 (Nov. 2014), pp. 2729–2742.

[5] X. Chen et al. "Sensor network security: a survey". In: *IEEE Commun. Surv. Tutorials* 11.2 (Feb. 2009), pp. 52–73.

[6] T. R. Jensen and B. Toft. *Graph coloring problems*. John Wiley & Sons, 2011.

[7] H. M. A. Kalyan Nakka. "An energy-efficient irregular hexagonal tessellation-based approach for connected k-coverage in planar wireless sensor networks". In: *AD hoc networks* 154 (2024), pp. 1–17.

[8] H. M. A. Kalyan Nakka. "Hierarchical Deployment and Square Tessellation for Connected k-Coverage in Heterogeneous Planar Wireless Sensor Networks". In: *ACM Trans. Sen. Netw* 21.2 (2025), pp. 1–27.

[9] J. Ko et al. "Wireless sensor networks for healthcare". In: *Proc. IEEE* 98.11 (2010), pp. 1947–1960.

[10] S. H. Lee et al. "Wireless sensor network design for tactical military applications: Remote large-scale environments". In: *MILCOM 2009-2009 IEEE Mil. commun. conf.* IEEE. Boston, USA, 2009, pp. 1–7.

[11] L. Lombardo et al. "Wireless sensor network for distributed environmental monitoring". In: *IEEE Trans. Instrum. Meas.* 67.5 (May 2017), pp. 1214–1222.

[12] Manju et al. "Proficient QoS-Based Target Coverage Problem in Wireless Sensor Networks". In: *IEEE Access* 8 (2020), pp. 74315–74325.

[13] P. Rawat et al. “Wireless sensor networks: a survey on recent developments and potential synergies”. In: *J. of Supercomput.* 68.1 (2014), pp. 1–48.

[14] L. Sau, P. Mukherjee, and S. C. Ghosh. “A Graph-Based Strategic Sensor Deployment Approach for k-Coverage in WSN”. In: *Adv. Inf. Netw Appl.* Ed. by L. Barolli. Cham: Springer Nature Switzerland, 2025, pp. 11–23.

[15] Y. Wang et al. “Coverage problem with uncertain properties in wireless sensor networks: A survey”. In: *Comput. Netw.* 123 (Aug. 2017), pp. 200–232.

iThenticate Page 56 of 56 - Integrity Submission Submission ID trn:oid:::3618:142751146